Release of labile Si from forest and agricultural soils

Artem Lim, Oleg S. Pokrovsky, Sophie S. Cornu, Jean-Dominique Meunier

Release of labile Si from forest and agricultural soils

Artem G. Lim[1], Oleg S. Pokrovsky[1,2,3*], Sophie Cornu[4], Jean-Dominique Meunier[4]

[1] *BIO-GEO-CLIM Laboratory, Tomsk State University, 36 Lenina Prs, 634050, Tomsk, Russia*

[2]*GET, CNRS - University of Toulouse, 14 Avenue Edouard Belin, 31400 Toulouse, France*

[3] *N. Laverov Federal Center for Integrated Arctic Research, UrB RAS, 23 Nab Severnoi Dviny, Arkhangelsk, 163000, Russia*

[4]*CEREGE, Aix-Marseille University, CNRS, IRD, INRAE, BP 80, 13545 Aix-en-Provence, France*

* oleg.pokrovsky@get.omp.eu

Submitted to *Catena* after revision, *May 2023*

Keywords: soil, forest, silicate, silica, dissolution, kinetics, rates, labile pool

Abstract

Despite the importance of silicon (Si) as benefecial nutrient for many plants, including economically-important cereals, the reactivity of various Si pools in soils (silicate minerals, amorphous compounds, phytoliths, organic litter) is not fully quantified which does not allow predicting the capacity of agricultural or forested soil to provide soluble Si to soil porewaters where it can be used by plants. Towards better understanding of factors controlling bioavailable Si in soils, here we quantified the release rate of Si from several pairs of French forest and agricultural topsoils, developed on calcareous or loess parent material. We used mixed-flow and column reactors, in acetate and carbonate buffers and distilled water, at various pH (4 to 8) and time of reaction (day to month).

The rate of Si release from soil (R_{Si}) exceeded that of crystalline clay minerals by 1 to 2 orders of magnitude, being 5 to 10 times lower than that of various allophanes. The rates were weakly dependent on pH (compared to clays or phytoliths) and varied from 5×10^{-7} to 2×10^{-6} $mol/g_{soil}/_{day}$ at $4 < pH \leq 8$. In terms of Si reactivity, four studied soil groups followed the order: "calcaric cambisols ≈ hypereutric cambisols ≥ luvisols ≥ albeluvisol". Calcaric and hypereutric cambisols as well as luvisols exhibited a weak decrease of R_{Si} with pH increase. The rate of Si release from albeluvisol increased 2 times with a pH increase from 4 to 8. There was no measurable difference in R_{Si} between agricultural and forest soils.

The pool of labile Si in forest soils was quantified via soil column flow-through experiments. The breakthrough curves of Si demonstrated high concentrations (1.6 to 5.7 mg/L) over first several hours of reaction in the soil column. The water leachable Si pool ranged from 0.04 to 0.08 mg Si g_{soil}^{-1}, corresponding to labile Si stock in the 0-20 cm soil of 80 to 160 kg ha^{-1}. These values can meet the annual requirements of plants in forests and cultivated soils. The pool of labile Si correlated ($R_{Pearson}$ >0.90; $p < 0.05$) with Si associated with amorphous Fe and Al compounds and soluble bioavailable Si extracted using $CaCl_2$

method, but negatively correlated with total Si content in soils and Si of phytoliths. The main pools of soil labile Si could be allophanes, organo-Fe-Al-Si compounds and adsorbed forms of Si onto Fe and Al hydroxides. We hypothesize that, because of low sensibility of R_{Si} to type of soil and fluid pH, the majority of soils regulate Si release at some 'universal' rate which is further reflected in relatively narrow range of riverine Si concentrations and export fluxes across the world. Therefore, the modeling of chemical weathering and element export flux in the watersheds should incorporate the experimentally measured reactivity of the whole soil rather than individual constituting primary or secondary minerals.

1. Introduction

Silicon is not seen as an essential element for plants, but many studies have documented that it is a beneficial element for many crops (Coskun et al., 2019). Low level of bioavailable Si has become an issue especially for cultivated soils naturally or anthropically depleted in plant available Si (Tubana et al. 2016; Haynes, 2017). The characterization of bioavailable soil Si is still empirical and the knowledge of fundamental mechanisms that drive the biogeochemical cycle of silica under cultivation are necessary for a better assessment of the impact of Si on plant development (Cooke and Leishman, 2016) as well as the future impact of global change on the Si cycle (Schaller et al., 2021; Yang et al., 2019, 2020).

There are several main reservoirs of Si in soils that can be used by plants provided that the Si leaching from these solid phases to the interstitial porewater is fast enough. First, these are primary and secondary crystalline silicate minerals that constitute the bulk of bottom and intermediate soil horizons. The reactivities (dissolution rates) of most Si-bearing primary and secondary alumosilicate minerals commonly present in soils and quartz are quite low (Schott et al., 2019) and not capable of providing sufficient amount of labile Si required for plant

growth, especially when the state of weathering is well advanced (de Tombeur et al., 2020). Possible exceptions are soils developed on highly reactive materials such as volcanic ash (Ugolini and Dahlgren, 2002; Vandekerkhove et al., 2016) or wollastonite (Cho et al., 2010). Amorphous materials, including biogenic silica (mainly phytoliths) and short-range order minerals have been identified as another potential source of dissolved Si (Puppe, 2015; Meunier et al., 2017; Cornu et al., 2022; Li et al., 2022). The reactivity of plant phytoliths is quite high, greatly exceeding that of clay minerals (Fraysse et al., 2009). The uptake of Si from phytoliths allows the plants to overcome labile Si deficit as it is established in various cultivated and pristine environments (Desplanques et al., 2005; De Tombeur et al., 2020; Gérard et al., 2008). Finally, the plant litter itself, where Si is present as both phytoliths and the dispersed form (Watteau and Villemin, 2001; Watteau et al., 2002; Fraysse et al., 2010), and Si which is bound to organic compounds (Kolesnikov and Gins, 2001), including humic acid-Al-Si complexes (Merdy et al., 2022) represent another potentially labile pool of Si for plants. For example, in the Amazonian forest, the Si input from the litterfall on top of the soil is about four times greater than the Si leached out of the system (Lucas et al., 1993).

In most soils, the Si pool available for plants may comprise all the reservoirs listed above. In addition, some Si can be adsorbed on the surfaces of soil minerals and organic debris and thus can be easily mobilized to aqueous solution (Rückert, 1992; Brinkman, 1970). However, aggregates in the soils may slower the process of dissolved Si mobilization (Li et al., 2022). So far, plant available Si (PAS) has been empirically estimated by chemical procedures using extractants such as 0.01 $CaCl_2$ (i.e., Haysom and Chapman, 1975) that provide a positive correlation with plant yield (Babu et al., 2016; Narayanaswamy and Prakash 2010). Various PAS quantification methods demonstrated positive correlations with factors that may affects Si availability, such as pedological and geological conditions (Landré et al., 2020), soil pH (Meunier et al., 2018; Caubet et al., 2020; Schaller et al., 2021), weathering stage (Klotzbücher

et al., 2014) and the presence of phytoliths (De Tombeur et al., 2020) and clay fraction and short-range ordered (SRO) aluminosilicates (e.g. allophanes and imogolites; Caubet et al., 2020; Cornu et al., 2022; Keller et al., 2021). Cornu et al (2022) found that PAS based on the $CaCl_2$ method was generally higher in cultivated soils than in forest soil and was controlled by pH and the presence of allophanes. However, the PAS methods do not allow to propose general laws of Si release rate. For this, laboratory experimental approaches are needed. Thus, Barao et al. (2019) used kinetic batch experiments with Belgium soils and found that reactivity of Si in croplands were higher than that of forest and pasture soils. Ronchi et al. (2015) used a leaching test approach on soil column to evaluate the dissolution rate of Si and to compare it with that of single soil minerals and biogenic Si pools. They found that the Si release from Belgian Luvisols and Sweden Cambisols are controlled by pH and decline from forest to cropland while PAS ($CaCl_2$ method) showed an opposite trend. Accordingly, more data is required to disentangle the significance of rate dissolution laws in soils and the impact on cultivated lands.

Building on this information, the purposes of this study are twofold. First, we aimed at assessing the rates of Si release from French temperate soils developed from calcareous or loess parent materials (characterized by Cornu et al., 2022), collected in adjacent cultivated and forest plots. Specifically, we intended to quantify the impact of solution composition (pH, presence of organic ligand or bicarbonate ion) on Si release rate in dynamic experiment and to compare Si release rate from various soils to that of clay minerals and Si-bearing amorphous compounds. Secondly, we focused on measuring initial, non-stationary Si release from soil, allowing to quantify the pool of most labile soil Si in order to relate it to conventionally-measured forms of Si in soils. In this regard, the present work is devoted to identify the physico-chemical (abiotic) factors controlling dynamic Si pool in soil. Furthermore, it allows quantifying possible bioavailable pool, rather than characterizing real bioavailability of silicon.

For the latter, specially designed mesocosm-level experiments with Si uptake by live plants and analysis of Si concentration in the biomass are necessary.

2. Materials and Methods

We have chosen seven French soils developed in calcareous or loess parent material in the temperate climate zone: 2 hypereutric cambisols (called 'calcisol' for brevity), 2 calcaric cambisols ('calcosol'), 2 luvisols, and 1 albeluvisol (WRB, 2006 soil classification; Chesworth et al., 2008). Their basic physical and chemical properties are listed in **Table 1** and more information is provided in Cornu et al. (2022). We used a paired site approach which includes adjacent soils with identical pedological factors (topography, parent material, climate and age) but different in their land use (cultivated versus forest soils). Localization of sampled soils is illustrated in Supplementary **Figure S1**. The soils were air dried, sieved through 2 mm sieve and sterilized prior to using for dissolution experiments. Specific surface area was measured using multiple point N_2 adsorption (Micrometrics ASAP 2010 apparatus) after degassing during 48 h at 120°C.

The experimental setup involved two independent dynamic (flow-through) reactors, operating at high and low ratio of fluid to soil (**Fig. 1**). In order to measure Si release rate from soils as a function of solution pH, at high fluid : solid ratio, we used classic mixed-flow reactor **(Fig. 1 A**), developed for measuring the dissolution rates of individual minerals (i.e., Pokrovsky et al., 2009, 2021; Schott et al., 2009). Similar reactors were used for assessing the Si-based reactivity of soil clay minerals (i.e., Köhler et al., 2003, 2005; Golubev et al., 2006), plant phytoliths (Fraysse et al., 2008, 2009) and whole plant litter (Fraysse et al., 2010). These reactors allow measuring steady-state Si release rate at fixed pH and other solution parameters. Steady-state dissolution rates were obtained at distinct solution compositions and

pH at a constant temperature of 25.0 ± 1.0°C in a thermostated room. Reacting fluids were comprised of deionized degassed H_2O, Merck reagent grade HCl, NaOH, $NaHCO_3$, $NaCH_3COO$, and NaCl. All solutions were prepared from 18 MΩ ultrapure sterile water (MilliQ Plus system) having a blank of dissolved organic carbon < 0.05 ppm. The input fluid was stored in a polyethylene container protected against CO_2 uptake from the atmosphere. It was injected into the reaction vessel using a Gilson® peristaltic pump at typical flow rates 0.1 mL min^{-1}. The reactor consisted of a 25 mL Teflon vessel which was continuously stirred with a floating Teflon supported magnetic stirrer, which prevented soil grinding during experiments. The reactive solution left the reactor through a series of 2.5 µm polycarbonate and 0.45 µm Nylon filters mounted in a row. All reactors initially contained 1.50 g of soil. The experiments started from injecting into reactor the Milli-Q water at pH = 5.6, followed by a mixture of 10 mM NaCl and 1 mM $NaHCO_3$ at pH = 8, and a mixture of 5 mM NaCl and 5 mM Acetic acid at pH = 4.2. The duration of each run ranged from 200 to 500 h. Finally, the reactor was run again with Milli-Q at pH around 6 during 450 h. For most experiments lasting 40-60 days in total, one sampling per day was performed. The total mass of soil in the reactor was measured at the beginning and at the end of experiment; no sizable changes (i.e., within 10 %) have been detected.

Steady-state dissolution rates (R_{Si}, mol g_{soil}^{-1} d^{-1}) were computed from measured solution composition using Eqn. 1:

$$R_{Si} = -q \cdot [Si(aq)]_{outlet} / m \quad (1)$$

where q (L s^{-1}) designates the fluid flow rate, $[Si(aq)]_{outlet}$ (mol L^{-1}) stands for the outlet Si concentration (M), and m (g) refers to the total soil mass of soil present in the reactor, respectively. Uncertainties on the steady-state rate constants are dominated by the uncertainty on the standard deviation on average Si a concentration at the steady-state (±10-20 %).

The second type of approach involved flow-through column experiments used for evaluating water-labile pool Si in soils (**Fig. 1 B**). Similar column experiments were shown to be efficient for measuring flux of Si from soils and assessing Si release rate at close to equilibrium conditions, at high soil : fluid ratio, most pertinent to natural settings (Ronchi et al., 2015). This setup involved small polypropylene column (diameter 1 cm, length 5 cm) packed with sieved (< 2 mm) soils. The column was filled with 1 g of upper 0-10 cm horizon of forest soil (F1) and 3 g of lower 20-30 cm horizon of forest soils (F2); we used hypereutric cambisol, calcaric cambisol and luvisol for these experiments. Fine soil sample (< 2 mm) was placed on the top of Teflon cotton supported by a porous (< 500 µm) Teflon disk; the outlet of the column was fitted with a 0.45 µm filter, and the fluid flow direction was from the bottom to the top. Similar to mixed-flow reactors, three inlet solutions were used in column experiments: Milli-Q water at pH = 5.6, a mixture of 10 mM NaCl and 1 mM $NaHCO_3$ at pH = 8, and a mixture of 5 mM NaCl and 5 mM Acetic acid at pH = 4.2. Continuous breakthrough curves of solutes were monitored from specific conductivity and pH measurements of the outlet fluid. These allowed integrating the amount of Si released from soil column as a function of time and over full duration of experiments. Similar approach for identifying the labile Si pool was used in batch experiments of other studies (e.g., Barao et al. 2019). Because the concentration of Si in the column outlet solution strongly decreased over the first 10-100 h to some steady-state concentrations (see section 3.2 below), while the pH was buffered by acetate or carbonate buffer, the labile (fast leachable) pool of Si in soil sample was calculated for discrete time interval (0-10 h and 10 – 100 h). For this, we numerically integrated the amount of released Si with 1 to 2 h step for the 0-10 h period and with 10 to 20 h step for the 10-100 h period and normalized the mass of released Si to the total amount of soil in the column.

The pH in the outlet solution was measured using a combination glass electrode (Mettler Toledo) calibrated with NIST buffers (pH 4.01, 6.865, 9.18 at 25°C), with an uncertainty of ± 0.01 units. Aqueous silica concentration was determined using Quadripole ICP MS Agilent 7500 ce, with an uncertainty of 2% and a detection limit of $3.6 \cdot 10^{-7}$ M. The quality of measurements was monitored by regular analysis of SLRS-5 certified sample (2.2 mg L^{-1} Si) and an in-house standard of 0.01 M NaCl with ten times lower Si concentration.

Statistical treatment of the data included mean values and their standard deviations (in case of replicates and for calculating the steady-state concentrations from 4 to 5 sampling points) and linear regressions. Pairwise (Pearson) correlations were used to assess the relationship between various forms of Si in soils as measured by standard techniques (e.g., Cornu et al., 2022) and the labile Si pool measured in the experiments. Further, a pairwise comparative analysis was run via non-parametric Mann-Whitney test (U-test) to detect the differences between Si release rate or Si pools in datasets of different soils. The level of significance was fixed at 0.05 (95% confidence level) to consider a result as statistically notable. All plots were built using MS Excel 2016 and the Statistica-12 software package (http://www.statsoft.com).

3. RESULTS

3.1. Long-term dissolution in mixed-flow (open) reactors

Results of 16 long-term (10 - 15 days each) soil dissolution experiments are listed in Table 2 and illustrated in **Fig. 2** for two forest and two agricultural soils. The steady state outlet Si concentrations were typically achieved after first 20 h corresponding to 5 residence times of the fluid in the reactor. In this regard, the chemical and mechanical steady-state were similar. The outlet Si concentration responded to the change of chemical composition and the

pH of the inlet fluid. Silica concentration increased in the order "Milli-Q (pH = 6.0 - 6.5) < 0.01 M $NaCl/NaHCO_3$ (pH = 8.0±0.2) < 0.01 M Na Acetate (pH = 4.2±0.1)". After 800 h of experiment, we injected again the MilliQ water, and in most cases, the outlet concentration of Si were within ±20-30% of the values obtained at the beginning of experiment.

The Si release rates (R_{Si}) calculated from steady-state outlet Si concentration (Eqn. 1) presented a weak dependence on solution pH which was, however, depended on the type of soils (**Fig. 3**). The hypereutric cambisol R_{Si} decreased by a factor of 1.6 when pH increased from 4.2 to 6.5, had a minimum at pH 6.5 and then stabilized at pH close to 8 (**Fig. 3 A**). The calcaric cambisol R_{Si} decreased by a factor of 2±0.5 from pH 4.2 to 7-8 (**Fig. 3 B**). The luvisol R_{Si} exhibited a minimum at pH around 6 (**Fig. 3 C**). Finally, the albeluvisol stood apart from all other soils and yielded a 2-fold increase in R_{Si} when the pH increased from 4.1 to 8.2 (**Fig. 3 D**). None of the studied soil yielded significant (Mann-Whitney test, $p < 0.05$) difference in Si release rate between forested and cultivated soils. The plot of all soils in log *R*si scale demonstrated overall weak dependence on pH (**Fig. 4**). When normalized to specific surface areas, the rates of Si release from various soils exhibited the order 'hypereutric cambisol < luvisol < calcaric cambisol ~ albeluvisol' (**Table 2**; **Fig. S2** of the Supplement).

3.2. Silicon leaching from soils in the column reactor experiments

The rates of Si release from forest soils were calculated from the Si concentration at steady-state (typically after 10-100 h of reaction) in the column experiments using Eqn. 1. The rates measured in column reactors are listed in **Table 3**. The rates ranged from 1.0×10^{-6} to 1.9×10^{-7} mol Si g^{-1} day^{-1} for 800 to 150 µg L^{-1} of dissolved Si output concentration. These values are fairly comparable with R_{Si} measured in mixed-flow reactors, when the ratio soil : fluid was one order of magnitude higher.

At the same time, the initial outlet Si concentrations over first 4 hours were very high, ranging from 4000 to 8000 µg L^{-1} (**Fig. 5**). Specifically, the outlet Si concentrations decreased from 6000 to 1000 µg L^{-1} over 10 h reaction with hypereutric cambisols, from 4000 to 1000 µg L^{-1} over 7 h for calcaric cambisol and from 8000 to 500 µg L^{-1} over 6 h with luvisol. The initial outlet Si concentrations corresponded to instantaneous, non-steady state R_{Si} around 10^{-5} mol Si g^{-1} day^{-1}. This is an order of magnitude higher than the rates at the steady state measured in both mixed-flow reactor and column experiments. The numerical integration of the breakthrough curve (i.e., Si concentration vs time over first 0-10 h of reaction) in the Milli-Q water allowed quantifying the pools of labile Si, equaled to 0.08±0.01 mg Si g $soil^{-1}$ for hypereutric cambisols and 0.040±0.002 mg Si g $soil^{-1}$ for luvisols. These numbers were calculated from the average of two samples for each soil (1166 (F1+F2) and BS2 (F1+F2) of hypereutric cambisol; 340 (F1+F2) and 62 (F1+F2) of luvisol). The calcaric cambisols demonstrated much longer tail of high outlet concentrations, persistent over 90 h of reaction; the overall labile Si for calcosoil 755 F1 is estimated as 0.145±0.02 mg Si g $soil^{-1}$, although the actual uncertainties may be much higher. This particular behavior of calcosol could be linked to progressively dissolving carbonate mineral grains that buffered the release of Si from relevant silicate pools.

For calcaric cambisol and hypereutric cambisol, approximately half of the labile pool was mobilized over first 0-10 h of reaction (**Table 4**). In contrast, > 90 % of labile Si pool in the luvisol was released over first 4 h of reaction or even faster, given insufficient temporal resolution at the beginning of experiments. This difference can be tentatively linked to the fact that the cambisol had much higher quantity of clay minerals compared to the luvisol.

3.3. Testing the link between experimental Si release rate, labile Si pool and analytical Si pools in soils

Based on recent study of various conventional analytical pools of Si in soils (Cornu et al., 2022, see their **Table 1**), we tested a correlation of these pools with experimentally measured Si release rates in mixed flow reactors and labile Si pools measured in the column experiments. For this, we used steady-state R_{Si} values from mixed-flow (**Table 2**) and flow-through column (**Table 3**) experiments, and pools of labile soil Si integrated over 0-10 and 10-100 h of reaction in column experiments at various pH (**Table 4**). In the latter case, the reason for considering independently these two time intervals is that they could correspond to two pools of leachable Si, as seen from the relevant breakthrough curves (**Fig. 5**). In contrast, after 100 h of reaction, there are steady-state Si release processes that can be better reflected by a stationary Si release rate (R_{Si}). There was no significant (at $p < 0.05$) correlation between Si release rate neither in mixed flow nor column reactor, and any conventional analytical forms of soil Si, including content of total Si, oxalate-, $CaCl_2$-, and dithionite-extracted Si and phytoliths in studied soils (**Table S1** and **Fig. S3** of the Supplement). However, the pools of labile Si quantified from column experiments on forest soils exhibited significant correlations ($p < 0.05$) with certain labile Si forms in soils (**Table 5**). The strongest correlations (R^2 = 0.94-0.98, $p < 0.01$) were observed between Si pool mobilized over 10-100 h reaction in the Milli-Q water or over 0-10 h in the acetate buffer and Si concentration in the form of allophones/imogolites as extracted by Tamm method (Si_O), which provides amorphous Fe/Al compounds (**Fig. 6 A, B**). The pool of labile Si released over 10-100 h in the acetate buffer strongly ($R^2 = 0.97$, $p < 0.01$) correlated with Si_{CaCl2} forms in soils (soluble, bioavailable Si extracted with $CaCl_2$), **Fig. 6 C**. Note that the correlations of different Si forms in soils determined in Cornu et al. (2022) with total (0-100 h) leachable pool of Si determined in column experiments were much lower than those for two fractional pools (0-10 and 10-100 h). The total chemical pool of Si in soils (Si_{tot}) strongly ($R^2 \geq 0.94$, $p < 0.01$) anti-correlated

with both acetate- and Milli-Q reacting pools determined in column experiments (**Fig. S4** of the Supplement).

4. DISCUSSION

4.1. Comparison of Si release rate between bulk soil, minerals, and phytoliths

A comparison of whole soil Si release rates with dissolution rates of common soil minerals and plant phytoliths measured in the mixed-flow reactor similar to the one used in this study is given in **Figure 4**. Added to this figure also the recent data for allophane dissolution in batch reactors (Ralston et al., 2018) and results of column leaching experiments on forest soils (Ronchi et al., 2015). Noteworthy that all soils except albeluvisol at pH 4.2 exhibited sizably higher (1-2 orders of magnitude) *R*si values compared to those of typical clay minerals present in soil. Whilst in acidic environment (pH = 4.0-4.5), the rates of Si release from the whole soil are 2 to 10 times higher than those of soil clay minerals, at pH = 6 to 8.5 the difference sizably increases because the clay minerals decrease their rates with pH between 4 < pH < 7.5. At the same time, this trend of R_{Si} with pH qualitatively corresponds to that observed for luvisols and hypereutric cambisols (calcisol) in **Fig. 3**. In contrast, the *R*si of French soils developed in calcareous or loess parent material stay essentially constant at (10 ± 5) × 10^{-6} mol Si /g_{soil}/day, or (8 ± 3) × 10^{-8} mol Si /m^2_{soil}/day. The calcaric cambisol (calcosol) and albeluvisol exhibited a different trend of R_{Si} with pH (Fig. 3). The dissolution rate of albeluvisol increases with pH, which is also observed for quartz given the importance of the quartz fraction in this type of soil, including the < 2 µm fraction (i.e., 60 % of the crystalline silicates, Cornu et al., 2022). However, the mass-normalized Si release rate from quartz is several orders of magnitude lower than that from studied soils, and the slope of log R_{Si} – pH

dependence for quartz is much higher than that observed for albulivisol (factor of 2 and 0.5 per one pH unit, respectively). Furthermore, the luvisol also contains sizable amount of quartz but did not yield an increase in R_{Si} with pH. For the calcaric cambisols (calcosol), there is a constant decrease of the dissolution rate with the pH. This could be due to a dissolution of the carbonate fraction in the first stage of the experiment.

Overall, at pH around 7-8, the difference in Si release rate between typical soil clay minerals and whole soils reaches more than 1.5-2.0 orders of magnitude. This is rather unexpected result, given that the synthetic clays (kaolinite, illite, chlorite and smectite) used for this plot constitute the majority of soils studied in this work (e.g., Cornu et al., 2022). However, one should be careful when performing such a comparison: individual clays used in previous experiments are generally better crystalline and larger than those encountered in soils. As a result, the mass-normalized reactivity of natural soil clays may be higher than those of synthetic crystalline minerals, as also demonstrated in some mineral bag natural experiments (e.g., Cornu et al., 1995).

The Si release rates from the whole soil measured in this study are drastically different from those of plant phytoliths as also shown in **Fig. 4**. Not only the plant phytoliths are 1 to 3 orders of magnitude more 'reactive' than soils (Fraysse et al., 2009), but the shapes of log R_{Si} - pH dependences between soils and phytoliths are totally different. Taken together, negligible role of phytoliths in Si supply to aqueous solution in experimental reactors and column-through experiments of the present study is demonstrated by lack of correlations (or negative correlations) between the labile Si pool and phytoliths content in forest soils (**Table 5**), and totally different pattern of rate dependence on solution pH for studied soils and plant phytoliths (**Fig. 4**). As such, the reactivity of Si in soils investigated in this study cannot be explained by a presence of small fraction of highly reactive phytoliths. In contrast to phytoliths, the plant litter exhibits quite weak dependence of R_{Si} on pH; for 6 various plants,

the Si release rate ranged from 10^{-7} to 10^{-5} mol g_{plant}^{-1} d^{-1} with very weak increase in R_{Si} with pH increase (ca., 0.3 log *R* unit per 5 pH unit, Fraysse et al., 2010). However, it is very unlikely that the presence of small (1-10%) amount of fresh, Si-rich plant litter in studied soils can explain their reactivity in aqueous solution: the content of refractory organic matter in soils is too low and highly variable among soils (10 to 70 g kg^{-1}, see **Table 1**) to allow a realistic impact of admixture of plant litter/soil humic material as a source of Si in aqueous solution contacting with soil in our experiments.

To get further insights into mechanisms driving Si release from soils in our experiments, we consider several possible pools of Si. First, in addition to poorly reactive quartz, these are 'primary' crystalline clays (kaolinite, illite, chlorite) and secondary, poorly crystalline smectites and/or interlayered illite-smectite minerals (Cornu et al., 2022). Second, there are amorphous/poorly crystalline imogolites and allophanes, including organo-alumino-siliceous, organo-Fe-Al-siliceous compounds (Farmer et al., 1980; Matichenkov and Snyder, 1996; Ralston et al., 2021). While the dissolution of 'usual' clays cannot provide the observed magnitude and pH-dependent pattern of R_{Si}, the reactivity of amorphous Si-bearing mineral and organo-mineral compounds such as pure end-member allophanes, including both Fe-free and Fe-rich compounds (i.e., Ralston et al., 2021) is an order of magnitude higher than that of soils studied in this work (see **Fig. 4**) and thus allophane cannot be excluded as a source of Si released from soils. An indirect evidence of the importance of this pool of soil Si in the short-term Si release patterns in our experiments is strong positive correlation observed between the labile Si assessed in column filtrations and Si_O measured by Tamm extraction procedure, and Si extractable by $CaCl_2$ (**Table 5, Fig. 6**). This is consistent with a similarity of the R_{Si} – pH dependence between allophanes and the calcaric cambisol, the soil in which allophane are the most present.

It has been known for long that silicic acid is readily adsorbed by and released from soils and soil minerals (Beckwirth and Reeve, 1963, 1964; McKeague and Cline, 1963; Haynes and Zhou, 2020). Therefore, the third major pool of soil Si is siliceous acid and silicate ions, adsorbed onto surfaces of soil minerals, first of all Al and Fe oxyhydroxides (Bruun Hansen et al., 1994; Hingston and Raupach, 1967). In particular, strong adsorption of Si onto $Fe(OH)_3$ is fairly well known (Dietzel et al., 2002; Vempati and Loeppert., 1989). The adsorption/desorption rate of silica from solid surfaces is usually very fast, and the equilibrium is established over the order of first hours (Beckwirth and Reeve, 1963, 1964). The majority of Si adsorbed on the surface of ferrihydrite and goethite at room temperature occurred over first 50 to 100 h (Delstanche et al., 2009). As such, the initial high Si concentration in flow-through column experiment can stem from mobilization of adsorbed Si pool. Consistent with this possibility is the observation that the reversible adsorption (and, consequently, desorption) of silicic acid onto/from Fe hydroxide is independent on pH at $5 \leq pH \leq 8$ (Sigg and Stumm, 1981).

Finally, a sizable pool of Si in soils may be represented by biogenic silica such as phytoliths, diatom frustules and exo-skeletons of protozoe (Sommer et al., 2006). The dissolution of this bulk biogenic silica, however, cannot provide the observed pH-independent pattern of Si release from soils studied in this work. In contrast to 'classic' phytolith such as those investigated by Fraysse et al (2006, 2009), small size phytogenic silica (< 5 μm, by definition proposed in Sommer et al., 2006) has not been investigated from the view point of its reactivity in aqueous solution. However, it is unlikely that both the magnitude and pH-dependence of small size phytogenic R_{Si} would be different from those of phytoliths: the grain size has no sizable impact on surface-normalized mineral dissolution rates, unless these minerals were subjected to strong shock which can generate dislocations (e.g., Schott et al., 2009). The same is true for abiotically formed amorphous silica which is known to precipitate

399 from soil solution in the form of pure phases on mineral surfaces (Drees et al., 1989): the
400 strongly pH-dependent pattern of amorphous silica dissolution rate is different from much
401 weaker pH dependence or even pH-independent pattern of Si release from soils, studied in
402 this work.

403 We observe a sizable, about two orders of magnitude, difference in Si release rate
404 measured for the French soils in the mixed-flow reactor in this study and the rates of Si
405 leaching in column experiments with forest and arable Swedish cambisols and Belgian
406 luvisols reported by Ronchi et al. (2015), **Fig. 4**. We tentatively explain this difference by
407 first, more important role of allophanes and less important role of clay minerals in controlling
408 Si release from studied soils compared to cambisols and luvisols of Ronchi et al. (2015). Note
409 that, although the rates of Si release from luvisol and hypereutric cambisol decrease with pH
410 similar to that of Ronchi et al. (2015), the R_{Si} measured in this study are 2.0±0.5 orders of
411 magnitude higher. Second, a lack of pH-dependence for Si release rate from soils in this study
412 (notably of calcaric cambisol and albeluvisol) and similarity of Si release rate in Ronchi et al
413 (2015) with common soil clays suggest the dominance of different mineral pools determining
414 the Si release pattern. In particular, we noted an order of magnitude higher $Si_{oxalate}$ content in
415 the soils of this study compared to those of Ronchi et al. (2015). Moreover, the initial outlet Si
416 concentration in experiments of Ronchi et al. (2015) was > 10 times higher than that in the
417 present study and it achieved 50 to 70 mg L^{-1}. At such high concentrations, the Si release
418 becomes limited by solubility of amorphous silica ($SiO_2 \times nH_2O$). It is thus possible that
419 mixed-flow reactors with high fluid:solid ratio, used in this study and the column reactors
420 with very low fluid:solid ratio of Ronchi et al (2015) do not probe the same pools of soil Si,
421 despite similar time scale used to extract the steady-state rates. Another possible explanation
422 could be linked to different nature and relative abundances of crystalline clays and short range
423 ordered minerals in soils used by these two studies.

4.2. Si release from soils in natural settings

Regardless of exact chemical and mineralogical nature of leachable Si pool in the studied soils, the main consequence of the presence of this labile Si is that it can be quickly, on the order of hours or even minutes, mobilized into aqueous solution (i.e., after rain infiltration) and become available for plant uptake. Overall, the pool of fast (0-10 and 10-100 h) water-leachable, mobile Si in forest soil ranges, depending on pH, from 0.04 mg Si g_{soil}^{-1} for luvisol to 0.08 mg Si g_{soil}^{-1} for hypereutric cambisol and calcaric cambisol (**Table 4**). Assuming that only upper 0-20 cm layer of soil reacts with aqueous solution (**Table 2**), and considering typical soil stock (0-20 cm) of 2×10^6 kg ha^{-1} (Winfried et al., 2018), this gives the labile Si stock of 80 to 160 kg bioavailable Si ha^{-1}. This value can meet the annual (or even monthly) requirements of plants in bioavailable Si (2 to 90 kg Si ha^{-1}, Cornelis et al., 2011; Cornelis and Delvaux, 2016). In the temperate forest, Si uptake flux by deciduous trees and Douglas fir ranges from 36 to 46 kg ha^{-1} y^{-1}, and that of the pine forest does not exceed 7 kg ha^{-1} y^{-1} (Lucas, 2001; Gérard et al., 2008). Therefore, experimentally measured mobile Si pool in forest soils is potentially capable of providing the totality of this demand; however, more measurements on specific soils are needed to further quantify this potential.

The upper (0-20 cm) soil profile can be considered as a mixed-flow reactor with rainwater input corresponding to annual precipitation minus evapotranspiration, or runoff of the riverine watershed. Combined with the mass of soil and the rates of labile Si release from bulk soil to the outlet river water, this allows determining the concentration C_{Si}:

$$C_{Si} = R_{Si} \times m / D \quad (2)$$

where m is the mass of soil in the ecosystem (kg ha^{-1}), D is the flow rate or annual runoff (precipitation minus evapotranspiration), in mm yr^{-1} or L ha^{-1}, and R_{Si} is the experimental dissolution rate (mol_{Si} g_{soil}^{-1} d^{-1}). To calculate C_{Si}, we will assume typical parameters of

449 temperate forest at the steady-state with respect to biomass growth and decay: $m_{0\text{-}20\ cm}$ = 200
450 kg m^{-2} or 2×10^6 kg ha^{-1} (Winfried et al., 2018), D = 13700 L d^{-1} ha^{-1} corresponding to a runoff
451 of 500 mm y^{-1}, and R_{Si} = 10^{-6} mol Si g_{soil}^{-1} d^{-1} corresponding to Si release rate from soil in
452 circumneutral solutions (pH = 5-8) measured in this study, see **Table 2** and **Fig. 4**. This yields
453 C_{Si} = 0.15 mol L^{-1} or 4100 mg Si L^{-1}, which is several orders of magnitude higher than typical
454 Si concentration in surface waters (4.2-5.0 mg L^{-1}, Gaillardet et al., 1999) and interstitial soil
455 solutions of surficial horizons (2.8 – 14 mg L^{-1}, Sommer et al., 2006; Pokrovsky et al., 2005a,
456 b). Therefore, less than 1% of upper soil, receiving the incoming rainwater and releasing Si at
457 the steady-state conditions (i.e., no aggrading forest and no silica precipitation in deeper parts
458 of the soil profile) is capable to provide the observed Si concentration in surface waters.
459 An unexpected result of this study is rather similar values of Si release rate regardless
460 of soil type, agricultural use, and solution pH. Note that we could not use coupled forest-
461 cultivable soil approach for quartz-rich and clay-poor sand dunes because agricultural soils
462 were not available for such substrates. It is thus possible that 'universal' Si release rate
463 proposed in this study might turn out to be not so 'universal' if screened across all possible
464 soils, including clay-poor sands or ultisols (red clay soils), which are dominated by 1:1 clay
465 minerals instead of 2:1 clays studied in this work. Therefore, keeping in mind that the
466 substrates investigated in this work are only representative for well differentiated soil
467 developed on loess and poorly differentiated soil developed on calcareous soils, we can
468 extend the discussion to more general case of various lithological context. We note that the
469 natural Si export fluxes (yields) by rivers from watersheds are also similar (by an order of
470 magnitude), despite large variations in soil type, rock lithology, vegetation, runoff and soil
471 solution pH across different biomes as illustrated below. Thus, the total annual Si export
472 fluxes by rivers of boreal and temperate watersheds, although sizably dependent on runoff,
473 are within the same order of magnitude regardless of climate and lithological context (basalts,

474 granites, sedimentary rocks and even peatland environments). For example, in boreal and
475 temperate zone, riverine Si yield ranges from 0.3 to 3.0 t Si km^{-2} y^{-1} (Oliva et al., 2003;
476 Zakharova et al., 2005, 2007; Pokrovsky et al., 2005b, 2020; Chupakov et al., 2020). A recent
477 study of 20 Canadian rivers of contrasting land cover, lithology, soil type and climate
478 demonstrated a range of Si export fluxes from 0.2 to 6.6 t km^{-2} y^{-1} with an average value of
479 1.6 t km^{-2} y^{-1} (Phillips and Cowling, 2019). Even in fresh Hawaiian basalts, the range of Si
480 export rate is only from 0.4 to 15 t km^{-2} y^{-1} (Derry et al., 2005), similar to silica export fluxes
481 from the rooting zone (20–30 cm depth) in these tropical settings (1.1 to 25 t km^{-2} y^{-1}, Hedin
482 et al., 2003). A compilation of 68 watersheds on granitoid rocks at highly contrasted runoff
483 and temperatures demonstrated a Si weathering flux that ranged within less than an order of
484 magnitude (White and Blum, 1995). The magnitude of these natural variations are much
485 lower than the ranges of Si release rates in laboratory experiments on various rocks and
486 individual minerals. Indeed, the laboratory-based dissolution rates of silicate minerals (R_{Si})
487 range over more than 4 orders of magnitude at circum-neutral pH, depending on the identity
488 of mineral (see Schott et al., 2009 and Heřmanská et al., 2022 for reviews). We therefore
489 hypothesize, that, in addition in incontestable control on Si export fluxes of transport
490 processes such as fluid residence time and flow rates (Maher, 2010) and biological processes
491 such as plant uptake and litter decay (Lucas et al., 1993; Derry et al., 2005; Gérard et al.,
492 2008; Fraysse et al., 2010), the topsoil itself may exert a major "buffering" effect on Si export
493 from the watershed. By virtue of its silicate minerals, notably short-range order clays, labile
494 Si pool and low sensibility of R_{Si} to the identity of soil and fluid pH, the soils across the world
495 may regulate Si release rate at some 'universal' rate which is further reflected in relatively
496 narrow range of riverine Si concentration and export flux. The latter is primarily dependent on
497 river runoff rather than soil type and land use of the watershed.

In this regard, reactive transport and biogeochemical modeling of Si (and related elements) cycle in the system 'rock-soil-river watershed' (i.e., Godderis et al., 2019) should incorporate the reactivity of soils based on experimental data of the whole soil rather than individual constituting minerals. Consideration of superposition of known dissolution rates of primary and secondary soil minerals, routinely used in such modeling, instead of experimentally-measured whole soil rates may underestimate Si release (and thus, relevant concentrations in surface fluids) by 1 to 2 orders of magnitude. As such, experimental measurements of labile Si in various soils across the world, using flow-through reactors with both soil powder and soil column are needed.

5. CONCLUDING REMARKS

Dynamic mixed-flow and column laboratory experiments of soil dissolution in aqueous solutions revealed similar behaviour for different type of soils developed on calcareous or loess parent materials (calcaric cambisol, hypereutric cambisol, albeluvisol and luvisol) suggesting similar mechanisms responsible for release of Si (R_{Si}) from the bulk of soil mineral matrix. The R_{Si} of studied soils was 1 to 2 orders of magnitude higher than that of common soil clays, and 1 to 3 orders of magnitude lower than that of plant phytoliths. Moreover, in contrast to clays and biogenic silica, the R_{Si} of whole soils weakly depended on pH at $4 < pH < 8$ (decreased by a factor 1.5 to 2 for hypereutric cambisol and calcaric cambisol; independent for luvisol, and increasing 2-fold for albeluvisol). As such, the two dominant 'bulk' pools of Si cannot explain the magnitude and pH-dependence of its release rate from soils. We hypothesize that either amorphous allophanes, imogolite, organo-Fe-Al-Si compounds (poorly known from the view point of dissolution kinetics), or Si desorption from common soil minerals (Fe and Al hydroxides) can be responsible for labile Si pool released from soil into aqueous solution. This pool of reactive Si amounted to 0.04-0.08 mg Si g_{soil}^{-1}

which is largely sufficient to provide the Si requirements of common plants in forest soils, and it can be mobilized into aqueous solution within first hours of contact with the fluid.

The reactivity of soils measured in this study demonstrates that very small fraction of actual soil present at the watershed (< 0.1-1%) is capable to provide the observed Si concentration in soil porewater and Si export flux from the watershed. Although we studied only limited number of soils, developed on loesses and calcareous substrates, we observed rather similar values of Si release rate regardless of the soil type, agricultural use, and solution pH. This may help to explain relatively low range of Si concentrations and fluxes observed in natural watersheds, compared to drastic differences in reactivity of individual silicate minerals or whole mother rocks inferred from laboratory experiments. Therefore, results obtained in the present study contribute to quantifying bulk soil reactivity with respect to Si release rate. We suggest that R_{Si} of whole soil, rather than that of individual soil minerals and amorphous (biogenic) silica, is better suited for being incorporated in existing reactive transport/chemical weathering models. This calls a need for experimental measurements of labile Si in various soils across the world, ideally using flow-through reactors.

Acknowledgements

Support from ANR BioSiSol is acknowledged. We thank A. Castillo for B.E.T. specific surface area measurements. OP and AL acknowledge support from the TSU Development Programme 'Priority-2030'.

REFERENCES

Babu, T., Tubana, B., Paye, W., Kanke, Y., Datnoff, L., 2016. Establishing Soil Silicon Test Procedure and Critical Silicon Level for Rice in Louisiana Soils. Commun. Soil Sci. Plant Anal. 47, 1578–1597. https://doi.org/10.1080/00103624.2016.1194996

Barão, L., Teixeira, R., Vandevenne, F., Ronchi, B., Unzué-Belmonte, D., Struyf, E., 2020. Silicon Mobilization in Soils: the Broader Impact of Land Use. Silicon 12, 1529–1538. https://doi.org/10.1007/s12633-019-00245-y

Beckwith, R.S., Reeve, R., 1964. Studies on soluble silica in soils. II. The release of monosilicic acid from soils. Soil Res. 2, 33–45. https://doi.org/10.1071/sr9640033

Beckwith, R.S., Reeve, R., 1963. Studies on soluble silica in soils. I. The sorption of silicic acid by soils and minerals. Soil Res. 1, 157. https://doi.org/10.1071/SR9630157
Blum, W.E.H., Schad, P., Nortcliff, S., 2018. Essentials of Soil Science Soil formation, functions, use and classification (World Reference Base, WRB). Schweizerbart Science Publishers, Stuttgart, Germany.
Brinkman, R., 1970. Ferrolysis, a hydromorphic soil forming process. Geoderma 3, 199–206. https://doi.org/10.1016/0016-7061(70)90019-4
Bruun Hansen, H.C., Raben-Lange, B., Raulund-Rasmussen, K., Borggaard, O.K., 1994. Monosilicate adsorption by ferrihydrite and goethite at pH 3–6. Soil Sci. 40–46. https://doi.org/10.1097/00010694-199407000-00005
Caubet, M., Cornu, S., Saby, N.P.A., Meunier, J.-D., 2020. Agriculture increases the bioavailability of silicon, a beneficial element for crop, in temperate soils. Sci. Rep. 10, 19999. https://doi.org/10.1038/s41598-020-77059-1
Chesworth, W., Camps Arbestain, M., Macías, F., Spaargaren, O., Spaargaren, O., Mualem, Y., Morel- Seytoux, H.J., Horwath, W.R., Almendros, G., Chesworth, W., Grossl, P.R., Sparks, D.L., Spaargaren, O., Fairbridge, R.W., Singer, A., Eswaran, H., Micheli, E., 2008. Classification of Soils: World Reference Base (WRB) for soil resources, in: Chesworth, W. (Ed.), Encyclopedia of Soil Science, Encyclopedia of Earth Sciences Series. Springer Netherlands, Dordrecht. https://doi.org/10.1007/978-1-4020-3995-9_104
Cho, Y., Driscoll, C.T., Johnson, C.E., Siccama, T.G., 2010. Chemical changes in soil and soil solution after calcium silicate addition to a northern hardwood forest. Biogeochemistry 3–20. https://doi.org/10.1007/s10533-009-9397-6
Chupakov, A.V., Pokrovsky, O.S., Moreva, O.Y., Shirokova, L.S., Neverova, N.V., Chupakova, A.A., Kotova, E.I., Vorobyeva, T.Y., 2020. High resolution multi-annual riverine fluxes of organic carbon, nutrient and trace element from the largest European Arctic river, Severnaya Dvina. Chem. Geol. 538, 119491. https://doi.org/10.1016/j.chemgeo.2020.119491
Cooke, J., Leishman, M.R., 2016. Consistent alleviation of abiotic stress with silicon addition: a meta-analysis. Funct. Ecol. 30, 1340–1357. https://doi.org/10.1111/1365-2435.12713
Cornelis, J.-T., Delvaux, B., 2016. Soil processes drive the biological silicon feedback loop. Funct. Ecol. 30, 1298–1310. https://doi.org/10.1111/1365-2435.12704
Cornelis, J.-T., Delvaux, B., Georg, R.B., Lucas, Y., Ranger, J., Opfergelt, S., 2011. Tracing the origin of dissolved silicon transferred from various soil-plant systems towards rivers: a review. Biogeosciences 8, 89–112. https://doi.org/10.5194/bg-8-89-2011
Cornu, S., Lucas, Y., Desjardins, T., Nitsche, S., 1995. Rapid weathering kinetics of secondary minerals in forest ferralsols of Central Amazonia: bag-mineral method. Comptes Rendus Acad. Sci. Ser. 2a Sci. Terre Planetes Fr. 311–316.
Cornu, S., Meunier, J.-D., Ratie, C., Ouedraogo, F., Lucas, Y., Merdy, P., Barboni, D., Delvigne, C., Borschneck, D., Grauby, O., Keller, C., 2022. Allophanes, a significant soil pool of silicon for plants. Geoderma 412, 115722. https://doi.org/10.1016/j.geoderma.2022.115722
Coskun, D., Deshmukh, R., Sonah, H., Menzies, J.G., Reynolds, O., Ma, J.F., Kronzucker, H.J., Bélanger, R.R., 2019. The controversies of silicon's role in plant biology. New Phytol. 221, 67–85. https://doi.org/10.1111/nph.15343
de Tombeur, F., Turner, B.L., Laliberté, E., Lambers, H., Mahy, G., Faucon, M.-P., Zemunik, G., Cornelis, J.-T., 2020. Plants sustain the terrestrial silicon cycle during ecosystem retrogression. Science 369, 1245–1248. https://doi.org/10.1126/science.abc0393

Delstanche, S., Opfergelt, S., Cardinal, D., Elsass, F., André, L., Delvaux, B., 2009. Silicon isotopic fractionation during adsorption of aqueous monosilicic acid onto iron oxide. Geochim. Cosmochim. Acta 73, 923–934. https://doi.org/10.1016/j.gca.2008.11.014

Derry, L.A., Kurtz, A.C., Ziegler, K., Chadwick, O.A., 2005. Biological control of terrestrial silica cycling and export fluxes to watersheds. Nature 433, 728–731. https://doi.org/10.1038/nature03299

Desplanques, V., Cary, L., Mouret, J.-C., Trolard, F., Bourrié, G., Grauby, O., Meunier, J.-D., 2006. Silicon transfers in a rice field in Camargue (France). J. Geochem. Explor. 88, 190–193. https://doi.org/10.1016/j.gexplo.2005.08.036

Dietzel, M., 2002. Interaction of polysilicic and monosilicic acid with mineral surfaces, in: Stober, I., Bucher, K. (Eds.), Water-Rock Interaction, Water Science and Technology Library. Springer Netherlands, Dordrecht, pp. 207–235. https://doi.org/10.1007/978-94-010-0438-1_9

Farmer, V.C., Russell, J.D., Berrow, M.L., 1980. Imogolite and Proto-Imogolite Allophane in Spodic Horizons: Evidence for a Mobile Aluminium Silicate Complex in Podzol Formation. J. Soil Sci. 31, 673–684. https://doi.org/10.1111/j.1365-2389.1980.tb02113.x

Fraysse, F., Pokrovsky, O.S., Meunier, J.D., 2010. Experimental study of terrestrial plant litter interaction with aqueous solutions. Geochim. Cosmochim. Acta 74, 70–84. https://doi.org/10.1016/j.gca.2009.09.002

Fraysse, F., Pokrovsky, O.S., Schott, J., Meunier, J.-D., 2009. Surface chemistry and reactivity of plant phytoliths in aqueous solutions. Chem. Geol. 258, 197–206. https://doi.org/10.1016/j.chemgeo.2008.10.003

Fraysse, F., Pokrovsky, O.S., Schott, J., Meunier, J.-D., 2006. Surface properties, solubility and dissolution kinetics of bamboo phytoliths. Geochim. Cosmochim. Acta 70, 1939–1951. https://doi.org/10.1016/j.gca.2005.12.025

Gaillardet, J., Dupré, B., Louvat, P., Allègre, C.J., 1999. Global silicate weathering and CO2 consumption rates deduced from the chemistry of large rivers. Chem. Geol. 159, 3–30. https://doi.org/10.1016/S0009-2541(99)00031-5

Gérard, F., Mayer, K.U., Hodson, M.J., Ranger, J., 2008. Modelling the biogeochemical cycle of silicon in soils: Application to a temperate forest ecosystem. Geochim. Cosmochim. Acta 72, 741–758. https://doi.org/10.1016/j.gca.2007.11.010

Goddéris, Y., Schott, J., Brantley, S.L., 2019. Reactive Transport Models of Weathering. Elements 15, 103–106. https://doi.org/10.2138/gselements.15.2.103

Golubev, S.V., Bauer, A., Pokrovsky, O.S., 2006. Effect of pH and organic ligands on the kinetics of smectite dissolution at 25°C. Geochim. Cosmochim. Acta 70, 4436–4451. https://doi.org/10.1016/j.gca.2006.06.1557

Haynes, R.J., 2017. Chapter Three - Significance and Role of Si in Crop Production, in: Sparks, D.L. (Ed.), Advances in Agronomy. Academic Press, pp. 83–166. https://doi.org/10.1016/bs.agron.2017.06.001

Haynes, R.J., Zhou, Y.-F., 2020. Silicate sorption and desorption by a Si-deficient soil – Effects of pH and period of contact. Geoderma 365, 114204. https://doi.org/10.1016/j.geoderma.2020.114204

Haysom, M.B.C., Chapman, L.S., 1975. Some aspects of the calcium silicate trials at Mackay. Proc Qld Soc Sugar Cane Technol 117–122.

Hedin, L.O., Vitousek, P.M., Matson, P.A., 2003. Nutrient losses over four million years of tropical forest development. Ecology 84, 2231–2255. https://doi.org/10.1890/02-4066

Heřmanská, M., Voigt, M.J., Marieni, C., Declercq, J., Oelkers, E.H., 2022. A comprehensive and internally consistent mineral dissolution rate database: Part I: Primary silicate

minerals and glasses. Chem. Geol. 597, 120807. https://doi.org/10.1016/j.chemgeo.2022.120807
Hingston, F.J., Raupach, M., 1967. The reaction between monosilicic acid and aluminium hydroxide. I. Kinetics of adsorption of silicic acid by aluminium hydroxide. Soil Res. 5, 295–309. https://doi.org/10.1071/sr9670295
Keller, C., Rizwan, M., Meunier, J.-D., 2021. Are clay minerals a significant source of Si for crops? A Comparison of amorphous silica and the roles of the mineral type and pH. Silicon 13, 3611–3618. https://doi.org/10.1007/s12633-020-00877-5
Klotzbücher, T., Marxen, A., Vetterlein, D., Schneiker, J., Türke, M., van Sinh, N., Manh, N.H., van Chien, H., Marquez, L., Villareal, S., Bustamante, J.V., Jahn, R., 2015. Plant-available silicon in paddy soils as a key factor for sustainable rice production in Southeast Asia. Basic Appl. Ecol. 16, 665–673. https://doi.org/10.1016/j.baae.2014.08.002
Köhler, S.J., Bosbach, D., Oelkers, E.H., 2005. Do clay mineral dissolution rates reach steady state? Geochim. Cosmochim. Acta 69, 1997–2006. https://doi.org/10.1016/j.gca.2004.10.015
Köhler, S.J., Dufaud, F., Oelkers, E.H., 2003. An experimental study of illite dissolution kinetics as a function of pH from 1.4 to 12.4 and temperature from 5 to 50°C. Geochim. Cosmochim. Acta 67, 3583–3594. https://doi.org/10.1016/S0016-7037(03)00163-7
Kolesnikov, M.P., Gins, V.K., 2001. Forms of silicon in medicinal plants. Appl. Biochem. Microbiol. 37, 524–527. https://doi.org/10.1023/A:1010262527643
Landré, A., Cornu, S., Meunier, J.-D., Guerin, A., Arrouays, D., Caubet, M., Ratié, C., Saby, N.P.A., 2020. Do climate and land use affect the pool of total silicon concentration? A digital soil mapping approach of French topsoils. Geoderma 364, 114175. https://doi.org/10.1016/j.geoderma.2020.114175
Li, Z., Meunier, J.-D., Delvaux, B., 2022. Aggregation reduces the release of bioavailable silicon from allophane and phytolith. Geochim. Cosmochim. Acta 325, 87–105. https://doi.org/10.1016/j.gca.2022.03.025
Lowson, R.T., Comarmond, M.-C.J., Rajaratnam, G., Brown, P.L., 2005. The kinetics of the dissolution of chlorite as a function of pH and at 25°C. Geochim. Cosmochim. Acta 69, 1687–1699. https://doi.org/10.1016/j.gca.2004.09.028
Lucas, Y., 2001. The role of plants in controlling rates and products of weathering: Importance of biological pumping. Annu. Rev. Earth Planet. Sci. 29, 135–163. https://doi.org/10.1146/annurev.earth.29.1.135
Lucas, Y., Luizao, F.J., Chauvel, A., Rouiller, J., Nahon, D., 1993. The relation between biological activity of the rain forest and mineral composition of soils. Science 260, 521–523. https://doi.org/10.1126/science.260.5107.521
Maher, K., 2010. The dependence of chemical weathering rates on fluid residence time. Earth Planet. Sci. Lett. 294, 101–110. https://doi.org/10.1016/j.epsl.2010.03.010
Matichenkov, V.V., Snyder, G.H., 1996. The mobile silicon compounds in some South Florida soils. Eurasian Soil Sci. 1165–1180.
McKeague, J.A., Cline, M.G., 1963. Silica in soil solutions: ii: the adsorption of monosilicic acid by soil and by other substances. Can. J. Soil Sci. 43, 83–96. https://doi.org/10.4141/cjss63-011
Merdy, P., Meunier, J.-D., Ziarelli, F., Lucas, Y., 2022. Evidence of humic acid-aluminium- silicon complexes under controlled conditions. Sci. Total Environ. 829, 154601. https://doi.org/10.1016/j.scitotenv.2022.154601
Meunier, J.D., Barboni, D., Anwar-ul-Haq, M., Levard, C., Chaurand, P., Vidal, V., Grauby, O., Huc, R., Laffont-Schwob, I., Rabier, J., Keller, C., 2017. Effect of phytoliths for

mitigating water stress in durum wheat. New Phytol. 215, 229–239. https://doi.org/10.1111/nph.14554
Meunier, J.-D., Colin, F., Alarcon, C., 1999. Biogenic silica storage in soils. Geology 27, 835–838. https://doi.org/10.1130/0091-7613.
Meunier, J.-D., Cornu, S., Keller, C., Barboni, D., 2022. The role of silicon in the supply of terrestrial ecosystem services. Environ. Chem. Lett. 20, 2109–2121. https://doi.org/10.1007/s10311-021-01376-8
Meunier, J.-D., Sandhya, K., Prakash, N.B., Borschneck, D., Dussouillez, P., 2018. pH as a proxy for estimating plant-available Si? A case study in rice fields in Karnataka (South India). Plant Soil 432, 143–155. https://doi.org/10.1007/s11104-018-3758-7
Narayanaswamy, C., Prakash, N.B., 2010. Evaluation of selected extractants for plant-available silicon in rice soils of Southern India. Commun. Soil Sci. Plant Anal. 41, 977–989. https://doi.org/10.1080/00103621003646063
Oliva, P., Viers, J., Dupré, B., 2003. Chemical weathering in granitic environments. Chem. Geol. 202, 225–256. https://doi.org/10.1016/j.chemgeo.2002.08.001
Phillips, A.K., Cowling, S.A., 2019. Biotic and abiotic controls on watershed Si cycling and river Si yield in western Canada. Biogeochemistry 143, 221–237. https://doi.org/10.1007/s10533-019-00557-6
Pokrovsky, O.S., Dupré, B., Schott, J., 2005a. Fe–Al–organic Colloids Control of Trace Elements in Peat Soil Solutions: Results of Ultrafiltration and Dialysis. Aquat. Geochem. 11, 241–278. https://doi.org/10.1007/S10498-004-4765-2
Pokrovsky, O.S., Manasypov, R.M., Kopysov, S.G., Krickov, I.V., Shirokova, L.S., Loiko, S.V., Lim, A.G., Kolesnichenko, L.G., Vorobyev, S.N., Kirpotin, S.N., 2020. Impact of permafrost thaw and climate warming on riverine export fluxes of carbon, nutrients and metals in Western Siberia. Water Switz. 12, 1817. https://doi.org/10.3390/w12061817
Pokrovsky, O.S., Schott, J., Kudryavtzev, D.I., Dupré, B., 2005b. Basalt weathering in Central Siberia under permafrost conditions. Geochim. Cosmochim. Acta 69, 5659–5680. https://doi.org/10.1016/j.gca.2005.07.018
Pokrovsky, O.S., Shirokova, L.S., Benezeth, P., Schott, J., Golubev, S.V., 2009. Effect of organic ligands and heterotrophic bacteria on wollastonite dissolution kinetics. Am. J. Sci. 309, 731–772. https://doi.org/10.2475/08.2009.05
Pokrovsky, O.S., Shirokova, L.S., Zabelina, S.A., Jordan, G., Benezeth, P., 2021. Weak impact of microorganisms on Ca, Mg-bearing silicate weathering. NPj Materials Degradation, 5, Art No 51. https://doi.org/10.1038/s41529-021-00199-w.
Puppe, D., Ehrmann, O., Kaczorek, D., Wanner, M., Sommer, M., 2015. The protozoic Si pool in temperate forest ecosystems — Quantification, abiotic controls and interactions with earthworms. Geoderma 243–244, 196–204. https://doi.org/10.1016/j.geoderma.2014.12.018
Ralston, S.J., Hausrath, E.M., Tschauner, O., Rampe, E., Peretyazhko, T.S., Christoffsen, R., Defelice, C., Lee, H., 2021. Dissolution rates of allophane with variable Fe contents: implications for aqueous alteration and the preservation of X-RAY amorphous materials on Mars. Clays Clay Miner. 69, 263–288. https://doi.org/10.1007/s42860-021-00124-x
Richard Drees, L., Wilding, L.P., Smeck, N.E., Senkayi, A.L., 1989. Silica in Soils: Quartz and Disordered Silica Polymorphs, in: Minerals in Soil Environments. John Wiley & Sons, Ltd, pp. 913–974. https://doi.org/10.2136/sssabookser1.2ed.c19
Ronchi, B., Barão, L., Clymans, W., Vandevenne, F., Batelaan, O., Govers, G., Struyf, E., Dassargues, A., 2015. Factors controlling Si export from soils: A soil column approach. Catena 133, 85–96. https://doi.org/10.1016/j.catena.2015.05.007

Ronchi, B., Clymans, W., Barão, A.L.P., Vandevenne, F., Struyf, E., Batelaan, O., Dassargues, A., Govers, G., 2013. Transport of Dissolved Si from Soil to River: A Conceptual Mechanistic Model. Silicon 5, 115–133. https://doi.org/10.1007/s12633-012-9138-7

Rozalén, M.L., Huertas, F.J., Brady, P.V., Cama, J., García-Palma, S., Linares, J., 2008. Experimental study of the effect of pH on the kinetics of montmorillonite dissolution at 25°C. Geochim. Cosmochim. Acta 72, 4224–4253. https://doi.org/10.1016/j.gca.2008.05.065

Rückert, E., 1992. Naßbleichung und Tonzerstörung durch Ferrolysis in Stauwasserböden Baden-Württembergs? Hohenheimer Bodenkundliche Hefte 3, 1–178.

Schaller, J., Puppe, D., Kaczorek, D., Ellerbrock, R., Sommer, M., 2021. Silicon Cycling in Soils Revisited. Plants 10, 295. https://doi.org/10.3390/plants10020295

Schott, J., Pokrovsky, O.S., Oelkers, E.H., 2009. The Link Between Mineral Dissolution/Precipitation Kinetics and Solution Chemistry. Rev. Mineral. Geochem. 70, 207–258. https://doi.org/10.2138/rmg.2009.70.6

Sigg, L., Stumm, W., 1981. The interaction of anions and weak acids with the hydrous goethite (α-FeOOH) surface. Colloids Surf. 2, 101–117. https://doi.org/10.1016/0166-6622(81)80001-7

Sommer, M., Kaczorek, D., Kuzyakov, Y., Breuer, J., 2006. Silicon pools and fluxes in soils and landscapes—a review. J. Plant Nutr. Soil Sci. 169, 310–329. https://doi.org/10.1002/jpln.200521981

Tubana, B.S., Babu, T., Datnoff, L.E., 2016. A Review of Silicon in Soils and Plants and Its Role in US Agriculture: History and Future Perspectives. Soil Sci. 181, 393. https://doi.org/10.1097/SS.0000000000000179

Ugolini, F.C., Dahlgren, R.A., 2002. Soil Development in Volcanic Ash. Glob. Environ. Res. 69–82.

Vandekerkhove, E., Bertrand, S., Reid, B., Bartels, A., Charlier, B., 2016. Sources of dissolved silica to the fjords of northern Patagonia (44–48°S): the importance of volcanic ash soil distribution and weathering. Earth Surf. Process. Landf. 41, 499–512. https://doi.org/10.1002/esp.3840

Vempati, R.K., Loeppert, R.H., 1989. Influence of Structural and Adsorbed Si on the Transformation of Synthetic Ferrihydrite. Clays Clay Miner. 37, 273–279. https://doi.org/10.1346/CCMN.1989.0370312

Watteau, F., Villemin, G., 2001. Ultrastructural study of the biogeochemical cycle of silicon in the soil and litter of a temperate forest. Eur. J. Soil Sci. 52, 385–396. https://doi.org/10.1046/j.1365-2389.2001.00391.x

Watteau, F., Villemin, G., Ghanbaja, J., Genet, P., Pargney, J.-C., 2002. In situ ageing of fine beech roots (Fagus sylvatica) assessed by transmission electron microscopy and electron energy loss spectroscopy: description of microsites and evolution of polyphenolic substances. Biol. Cell 94, 55–63. https://doi.org/10.1016/S0248-4900(02)01182-6

White, A.F., Blum, A.E., 1995. Effects of climate on chemical_ weathering in watersheds. Geochim. Cosmochim. Acta 59, 1729–1747. https://doi.org/10.1016/0016-7037(95)00078-E

Yang, S., Hao, Q., Liu, H., Zhang, X., Yu, C., Yang, X., Xia, S., Yang, W., Li, J., Song, Z., 2019. Impact of grassland degradation on the distribution and bioavailability of soil silicon: Implications for the Si cycle in grasslands. Sci. Total Environ. 657, 811–818. https://doi.org/10.1016/j.scitotenv.2018.12.101

Yang, X., Song, Z., Yu, C., Ding, F., 2020. Quantification of different silicon fractions in broadleaf and conifer forests of northern China and consequent implications for

biogeochemical Si cycling. Geoderma 361, 114036. https://doi.org/10.1016/j.geoderma.2019.114036
Zakharova, E.A., Pokrovsky, O.S., Dupré, B., Gaillardet, J., Efimova, L.E., 2007. Chemical weathering of silicate rocks in Karelia region and Kola peninsula, NW Russia: Assessing the effect of rock composition, wetlands and vegetation. Chem. Geol. 242, 255–277. https://doi.org/10.1016/j.chemgeo.2007.03.018
Zakharova, E.A., Pokrovsky, O.S., Dupré, B., Zaslavskaya, M.B., 2005. Chemical weathering of silicate rocks in Aldan Shield and Baikal Uplift: insights from long-term seasonal measurements of solute fluxes in rivers. Chem. Geol. 214, 223–248. https://doi.org/10.1016/j.chemgeo.2004.10.003

Table 1. Soil origin, description, physical and chemical properties. More information is provided in Cornu et al. (2022). The soils are ordered as following: first the soil developed in calcareous rock containing carbonates, then those in which carbonates were dissolved, then soils developed in loess, with the most evolved at the end (albeluvisol). SOC is Soil Organic Carbon and SSA is Specific Surface Area.

Soil type (WRB, 2006)	**Sample I.D.**	**Sampling depth, cm (*)**	**SOC, g kg^{-1} (*)**	**pH (*)**	**< 2 µm g kg^{-1} (*)**	**SSA, m^2/g**
Calcaric Cambisol	701C1	0-20	47	7.9	491	
	701F1	0-20	53	6.8	477	
Calcaric Cambisol	755C1	0-20	23	8.1	514	49.1
	755F1	0-10	69	6.9	695	22.8
	755F2	10-20	39	7.7	514	
Hypereutric Cambisol	BS2C1	0-25	14	8.1	307	17.8
	BS2F1	0-10	39	5.9	282	14.2
	BS2F2	10-25	24	6.1	307	
Hypereutric Cambisol	1166C1	0-25	17	7.3	341	19.2
	1166F1	0-5	45	6.9	376	19.2
	1166F2	5-20	25	6.9	371	

Luvisol	340C1	0-25	11	7.0	156	12.6
	340F1	0-10	23	5.1	136	22.8
	340F2	10-25	11	5.0	134	
Luvisol	62C1	0-25	11	8.0	195	8.05
	62F1	0-5	29	4.1	162	6.11
	62F2	5-35	9.6	4.4	152	
Albeluvisol	BS3C1	0-20	9.5	7.1	160	10.5
	BS3F1	0-15	24	5.3	110	13.5
	BS3F2	15-25	12	4.9	108	

828

829 (*) Cornu et al. (2022)

830

831

Table 2. Si-based dissolution rates of soils determined in mixed-flow reactors. Here and below, bicarbonate is 10 mM NaCl +1 mM $NaHCO_3$; acetate is 5 mM NaCl+5 mM acetic acid. The pH values are measured in the outlet solutions, which corresponds to the steady-state conditions of the dissolution process.

Soil type	Fluid	Duration, h	pH	R_{Si}, mol/g_{soil}/h	S.D. R_{Si}	R_{Si}, mol/m^2/d	S.D. R_{Si}
Calcaric cambisol 701C1	MQ	260	7.13	4.6×10^{-8}	1.2×10^{-8}	-	-
	Bicarbonate	120	7.74	4.5×10^{-8}	3.4×10^{-9}	-	-
	Acetate	132	4.29	1.1×10^{-7}	4.2×10^{-9}	-	-
Calcaric cambisol 701F1	MQ	260	6.72	2.7×10^{-8}	6.6×10^{-9}	-	-
	Bicarbonate	120	7.76	3.8×10^{-8}	3.9×10^{-9}	-	-
	Acetate	132	4.2	5.2×10^{-8}	1.8×10^{-9}	-	-
Calcaric cambisol 755C1	MQ	288	6.41	8.6×10^{-8}	6.5×10^{-9}	1.2×10^{-8}	2.9×10^{-9}
	Bicarbonate	204	7.84	7.3×10^{-8}	1.4×10^{-9}	3.6×10^{-8}	6.8×10^{-9}
	Acetate	312	4.25	1.2×10^{-7}	1.5×10^{-8}	6.1×10^{-8}	7.4×10^{-9}
	MQ	144	6.78	6.3×10^{-8}	3.5×10^{-9}	3.1×10^{-8}	1.7×10^{-9}
Calcaric cambisol 755F1	MQ	288	6.86	5.3×10^{-8}	3.6×10^{-9}	5.6×10^{-8}	3.8×10^{-9}
	Bicarbonate	204	7.78	5.9×10^{-8}	5.9×10^{-9}	6.2×10^{-8}	6.2×10^{-9}
	Acetate	312	4.27	1.2×10^{-7}	4.4×10^{-9}	1.3×10^{-7}	4.6×10^{-9}
	MQ	504	5.88	8.1×10^{-8}	1.2×10^{-8}	8.5×10^{-8}	1.3×10^{-8}
Hypereutric cambisol BS2C1	MQ	228	6.43	6.5×10^{-8}	3.1×10^{-9}	1.1×10^{-7}	5.3×10^{-9}
	Bicarbonate	216	7.78	6.4×10^{-8}	5.6×10^{-9}	1.1×10^{-7}	9.5×10^{-9}
Hypereutric cambisol BS2F1	MQ	228	6.62	7.4×10^{-8}	7.2×10^{-9}	1.2×10^{-7}	1.2×10^{-8}
	Bicarbonate	288	7.93	7.2×10^{-8}	8.6×10^{-9}	1.2×10^{-7}	1.4×10^{-8}
	Acetate	120	4.43	1.1×10^{-7}	1.2×10^{-8}	1.8×10^{-7}	2.1×10^{-8}
	MQ	96	6.41	5.1×10^{-8}	5.2×10^{-9}	8.6×10^{-8}	8.7×10^{-9}
Hypereutric cambisol 1166C1	MQ	288	6.59	6.3×10^{-8}	9.6×10^{-9}	7.9×10^{-8}	1.2×10^{-8}
	Bicarbonate	204	7.83	6.5×10^{-8}	1.2×10^{-8}	8.2×10^{-8}	1.5×10^{-8}
	Acetate	312	4.25	9.1×10^{-8}	5.8×10^{-9}	1.1×10^{-7}	7.3×10^{-9}
Hypereutric cambisol 1166F1	MQ	288	6.56	4.9×10^{-8}	4.7×10^{-9}	6.1×10^{-8}	5.8×10^{-9}
	Bicarbonate	204	7.91	6.7×10^{-8}	4.4×10^{-9}	8.4×10^{-8}	5.5×10^{-9}
	Acetate	312	4.26	8.7×10^{-8}	2.4×10^{-9}	1.1×10^{-7}	2.9×10^{-9}
	MQ	504	5.74	6.1×10^{-8}	6.7×10^{-9}	7.6×10^{-8}	8.4×10^{-9}
Luvisol 340F1	MQ	288	6.17	3.5×10^{-8}	1.2×10^{-9}	3.7×10^{-8}	1.3×10^{-9}
	Bicarbonate	204	7.85	4.7×10^{-8}	2.6×10^{-9}	4.9×10^{-8}	2.8×10^{-9}
	Acetate	24	4.29	5.7×10^{-8}	3.8×10^{-9}	6.1×10^{-8}	3.9×10^{-9}
	MQ	312	5.57	4.4×10^{-8}	3.1×10^{-9}	4.6×10^{-8}	3.2×10^{-9}
Luvisol 340C1	MQ	24	6.27	4.4×10^{-8}	5.2×10^{-9}	8.3×10^{-8}	9.9×10^{-9}
	Bicarbonate	12	7.93	6.4×10^{-8}	4.1×10^{-9}	1.2×10^{-7}	7.8×10^{-9}
	Acetate	24	4.26	1.1×10^{-7}	4.2×10^{-9}	2.1×10^{-7}	8.1×10^{-9}
	MQ	312	5.74	4.2×10^{-8}	9.5×10^{-9}	7.9×10^{-8}	1.8×10^{-9}
Luvisol 62C1	MQ	228	6.52	6.3×10^{-8}	5.8×10^{-9}	1.9×10^{-7}	1.7×10^{-8}
	Bicarbonate	288	7.84	6.5×10^{-8}	4.5×10^{-9}	1.9×10^{-7}	1.3×10^{-8}
Luvisol	MQ	228	5.97	5.3×10^{-8}	1.9×10^{-8}	2.1×10^{-7}	7.6×10^{-8}

62F1	Bicarbonate	288	7.89	6.8×10^{-8}	4.6×10^{-8}	2.7×10^{-7}	6.3×10^{-8}
	Acetate	120	4.38	6.2×10^{-8}	2.4×10^{-9}	2.4×10^{-7}	9.2×10^{-9}
	MQ	96	6.16	2.8×10^{-8}	7.3×10^{-9}	1.1×10^{-7}	2.9×10^{-8}
Albeluvisol BS3C1 N50g	MQ	260	6.03	2.1×10^{-8}	4.8×10^{-9}	2.9×10^{-9}	6.9×10^{-10}
	Bicarbonate	120	7.9	4.5×10^{-8}	5.6×10^{-9}	6.4×10^{-9}	7.9×10^{-10}
	Acetate	132	4.1	2.5×10^{-8}	1.6×10^{-9}	3.6×10^{-9}	2.3×10^{-10}
Albeluvisol BS3F2 N37g	MQ	260	5.68	2.3×10^{-8}	3.8×10^{-9}	2.9×10^{-9}	4.7×10^{-10}
	Bicarbonate	120	8.16	3.8×10^{-8}	9.5×10^{-9}	4.8×10^{-9}	1.2×10^{-9}
	Acetate	132	4.11	1.9×10^{-8}	1.5×10^{-8}	2.5×10^{-9}	1.9×10^{-9}
Albeluvisol BS3F1 N47g	MQ	260	5.51	1.7×10^{-8}	3.4×10^{-9}	1.9×10^{-9}	3.8×10^{-10}
	Bicarbonate	120	8.14	3.5×10^{-8}	6.2×10^{-9}	3.9×10^{-9}	6.9×10^{-10}
	Acetate	132	4.06	2.8×10^{-8}	1.4×10^{-9}	3.1×10^{-10}	1.6×10^{-10}

Footnote : MQ is for Milli-Q, distilled water.

Table 3. Si release rates (mean ± s.d.) determined in column-through experiments.

Soil type	Fluid	Duration, h	pH outlet	R_{Si}, mol g_{soil}^{-1} d^{-1}
Calcaric cambisol	Milli-Q	240	6.26	$(3.7\pm2.3)\times10^{-8}$
755 F1 (0.5 g) + 755 F2 (1.5 g)	Acetate	100	4.20*	$(6.5\pm0.79)\times10^{-8}$
Hypereutric cambisol	Milli-Q	170	5.85	$(1.2\pm0.57)\times10^{-8}$
1166 F1 (1 g) + 1166 F2 (3g)	Acetate	190	4.42	$(5.3\pm1.4)\times10^{-8}$
Hypereutric cambisol BS2 F1(1 g) + BS2 F2 (3g)	Milli-Q	170	5.07	$(1.7\pm1.4)\times10^{-8}$
Luvisol	Milli-Q	170	5.26	$(6.9\pm6.8)\times10^{-9}$
340 F1 (1 g) +	Acetate	190	4.05	$(1.1\pm0.19)\times10^{-8}$
340 F2 (3 g)	Bicarbonate	390	7.95*	$(1.8\pm0.35)\times10^{-9}$
Luvisol	Milli-Q	170	4.58	$(7.7\pm5.5)\times10^{-9}$
62 F1 (1 g) +	Acetate	190	3.97	$(1.1\pm0.18)\times10^{-8}$
62 F2 (3 g)	Bicarbonate	390	8.10*	$(2.6\pm2.2)\times10^{-9}$

* Approximated based on results of mixed-flow reactors.

Table 4. Pools (mean ± s.d.) of labile, fast-leaching Si determined by integration of Si breakthrough curves in soil column experiments over the first 100 h of reaction.

Soil type	Fluid	Time, h	pH outlet	Pool $_{Si}$, mg kg_{soil}^{-1}
Calcaric cambisol 755 F1 (0.5 g) + 755 F2 (1.5 g)	MQ	0-10	6.47	45±8.7
		10-100	6.11	100±15
	Acetate	0-10	4.1*	103±70
		10-100	4.2*	83±4.9
Hypereutric cambisol 1166 F1(1 g) + 1166 F2 (3g)	MQ	0-10	6.75	48±5.5
		10-100	5.46	36±5.8
	Acetate	0-10	5.02	63±32
		10-100	4.06	106±10
Hypereutric cambisol BS2 F1 (1 g) + BS2 F2 (3 g)	MQ	0-10	5.25	40±7.9
		10-100	4.98	31±3.7
Luvisol 340 F1 (1 g) + F2 (3 g)	MQ	0-10	5.7	34±13
		10-100	5.15	11±2.1
	Acetate	0-10	4.16	3.0±0.7
		10-100	3.98	21±1.8
	Bicarbonate	0-10	7.85*	4.3±2.4
		10-100	7.95*	5.1±0.9
Luvisol 62 F1 (1 g) + F2 (3 g)	MQ	0-10	4.5	39±15
		10-100	4.62	19±2.5
	Acetate	0-10	3.98	2.4±0.6
		10-100	3.98	15±1.8
	Bicarbonate	0-10	7.9*	6.2±4.2
		10-100	8.1*	21±0.9

* Approximated based on results of mixed-flow reactors.

Table 5. Linear (Pearson) correlation matrix of pools of labile, fast-leaching Si and different Si forms in soils taken from Cornu et al. (2022). Significant correlations at $p < 0.01$, labelled by asterisk.

Time period, h	Si_{tot} (1)	Si_O (2)	Si_d (3)	Si_{CaCl2} (4)	Phytoliths
MQ 0-10 h	-0.72	0.73	0.68	0.94	-0.32
MQ 10-100 h	-0.98*	0.97*	0.93	0.73	-0.40
Acetate 0-10 h	-0.98*	0.99*	0.85	0.92*	-0.60
Acetate 10-100 h	-0.75	0.78	0.55	0.98*	-0.67

Footnote:

(1) Si_{tot}, total Si content in the soil, including quartz, and all mineral and amorphous forms
(2) Si_O, poorly crystalline Fe oxides and short-range ordered aluminosilicates such as allophanes and imogolites which were extracted by the oxalate method
(3) Si_d, iron oxides extracted by the dithionite-citrate-bicarbonate method
(4) Si_{CaCl2}, soluble and bioavailable Si, extracted using the $CaCl_2$ method

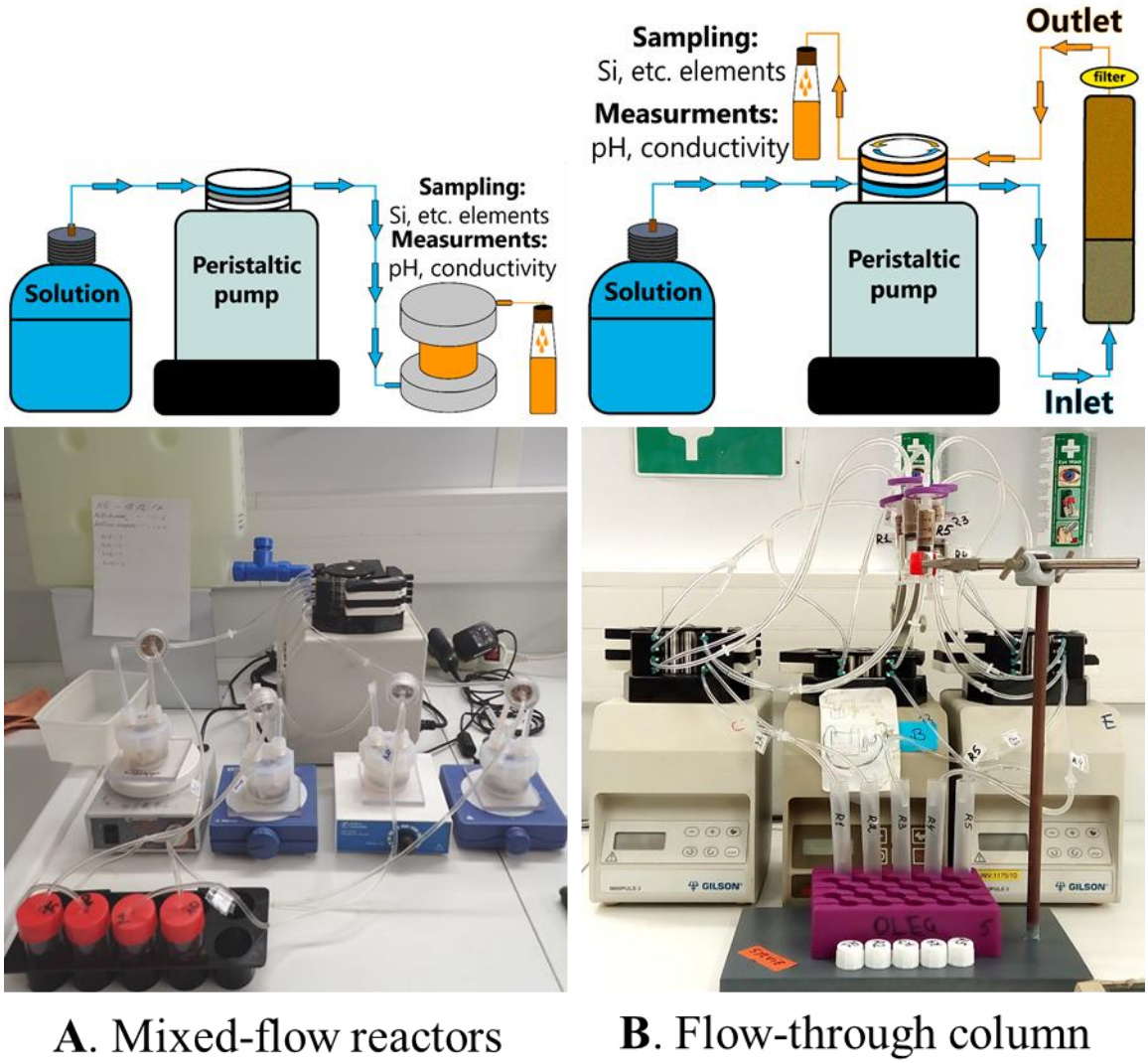

Figure 1. Experimental setup of mixed-flow reactors used for measurement of Si release rate from soils as a function of time and solution pH (A) and flow-through column experiments used for evaluating water-labile pool of adsorbed Si (B).

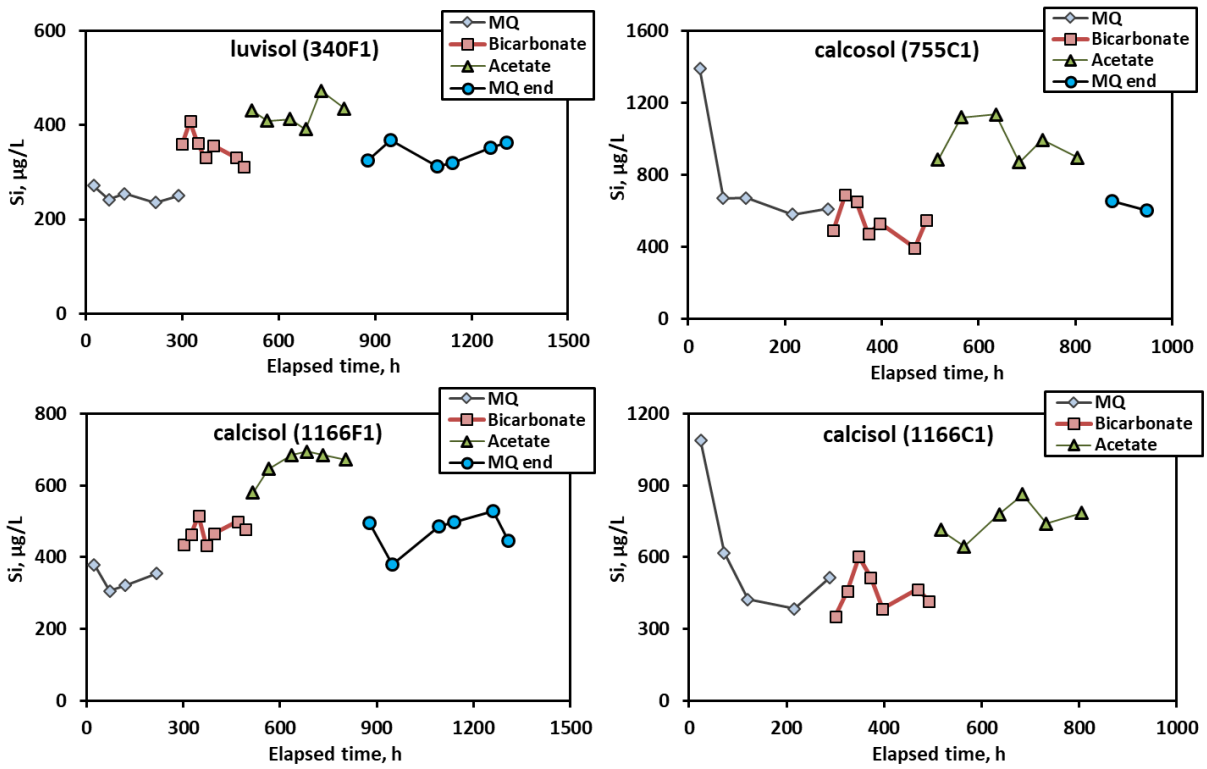

Figure 2. Examples of Si release pattern from different soils as a function of time, for different inlet solutions in the mixed-flow reactor. The inlet solutions were represented Milli-Q water at pH = 5.6, a mixture of 10 mM NaCl and 1 mM $NaHCO_3$ at pH = 8, and a mixture of 5 mM NaCl and 5 mM Acetic acid at pH = 4.2. The outlet pH values are listed in Table 2. For brevity, calcisol is used for hypereutric Cambisol and calcosol is for calcaric Cambisol.

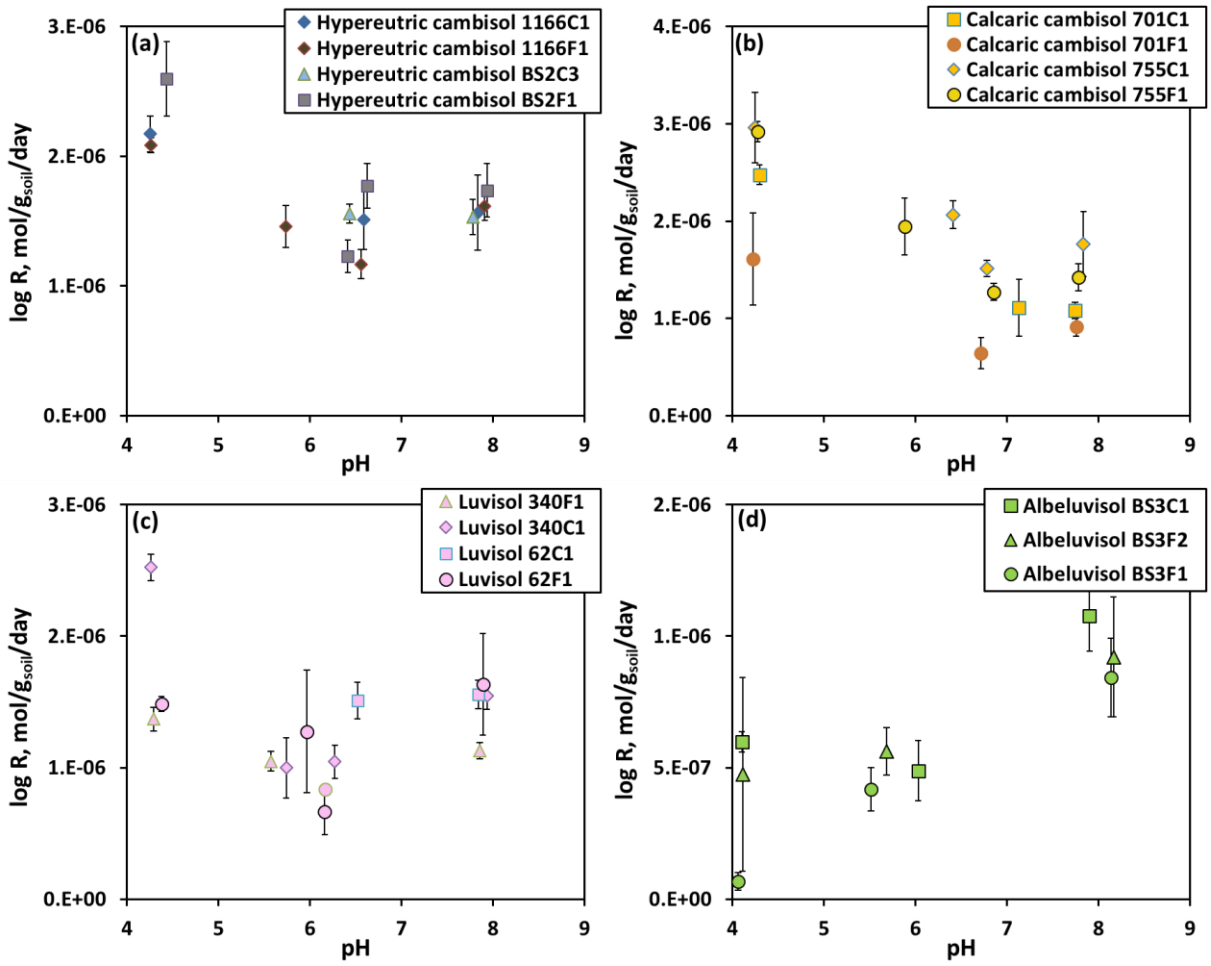

Fig. 3. Si release rate from couple cultivated-forest soils hypereutric cambisol **(A)**, calcaric cambisol **(B)**, luvisol **(C)** and albeluvisol **(D)** in mixed-flow reactors plotted as a function of outlet solution pH.

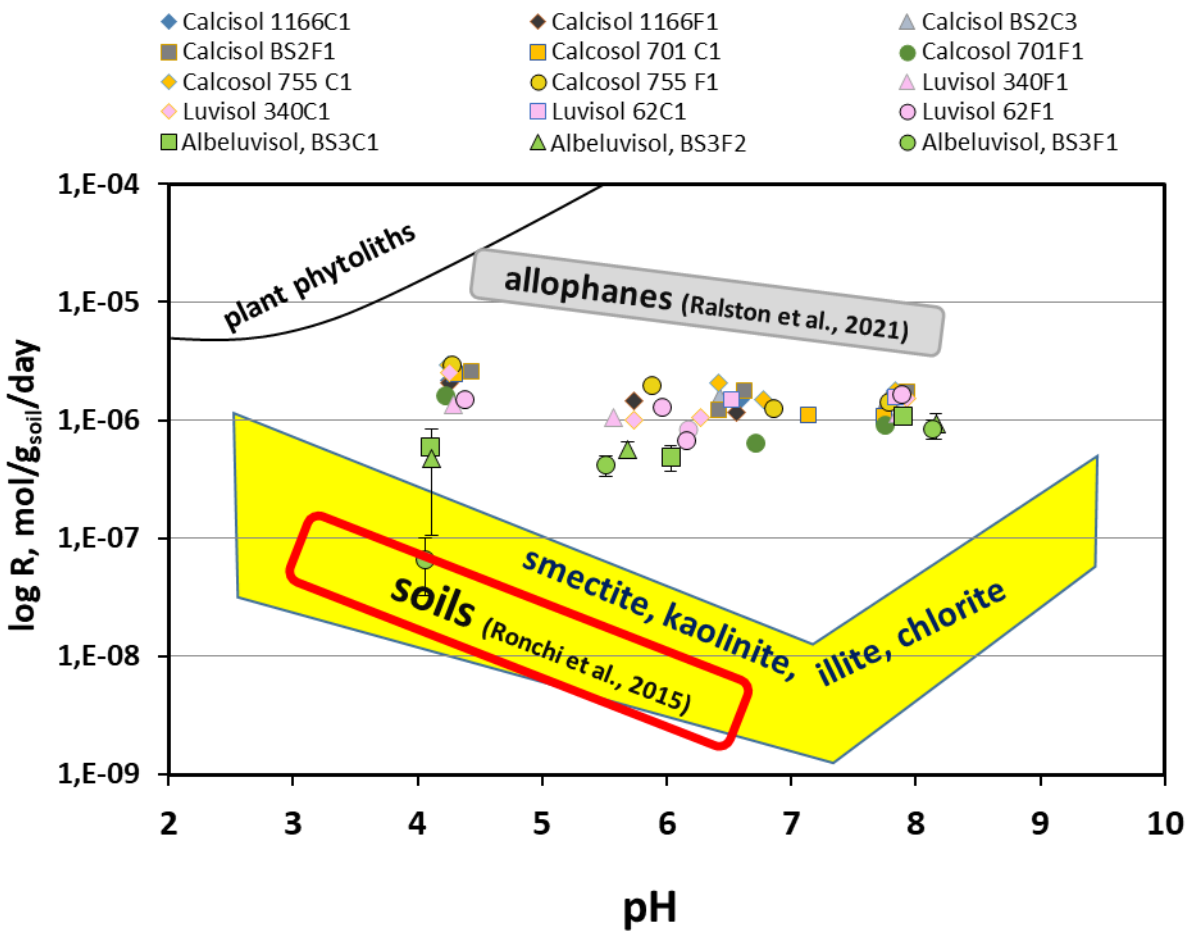

969
970

971 **Figure 4.** Si release rates for typical soil clay minerals and studied soils as a function of pH at
972 25°C. Soil clays are represented by smectite (Golubev et al., 2006; Rozalen et al., 2008),
973 kaolinite and illite (Köhler et al., 2003, 2005) and chlorite (Lowson et al., 2005). Black solid
974 line represents dissolution rate of various plant phytoliths (horsetail, larch, fern) taken from
975 Fraysse et al. (2009). Red rectangle marks the range of Si release rate from columns with
976 forest and arable cambisols and luvisols (Ronchi et al., 2015). Grey rectangles denotes the
977 range of Si release rate of allophanes (Ralston et al., 2021).

978

979

980

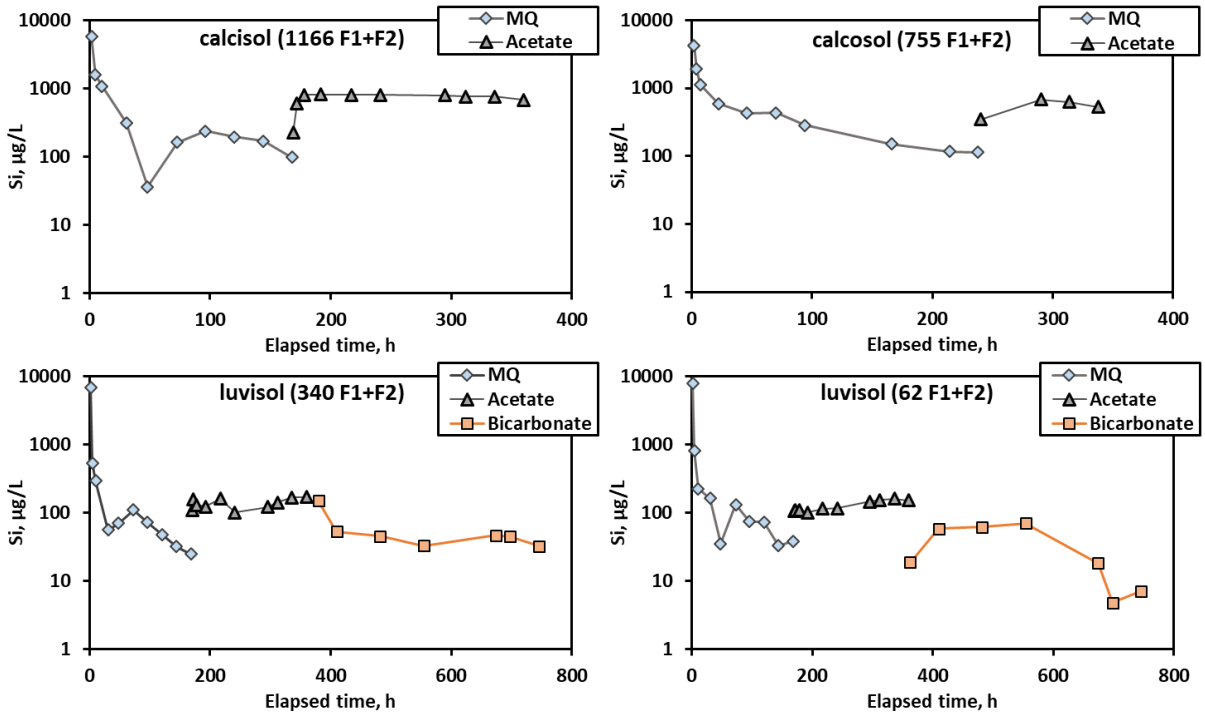

Figure 5. Examples of silica breakthrough curves in column experiments containing 1 g of surface and 3 g of intermediate horizons of forest soils. The initial (0-100 h) part of the curve was used to quantify the pool of water-labile Si present in the soil. For brevity, calcisol is used for the hypereutric Cambisol and calcosol denotes the calcaric Cambisol. Three inlet solutions were used in column experiments: Milli-Q water at pH = 5.6, a mixture of 10 mM NaCl and 1 mM NaHCO3 at pH = 8, and a mixture of 5 mM NaCl and 5 mM Acetic acid at pH = 4.2. The outlet pH is listed in Table 3.

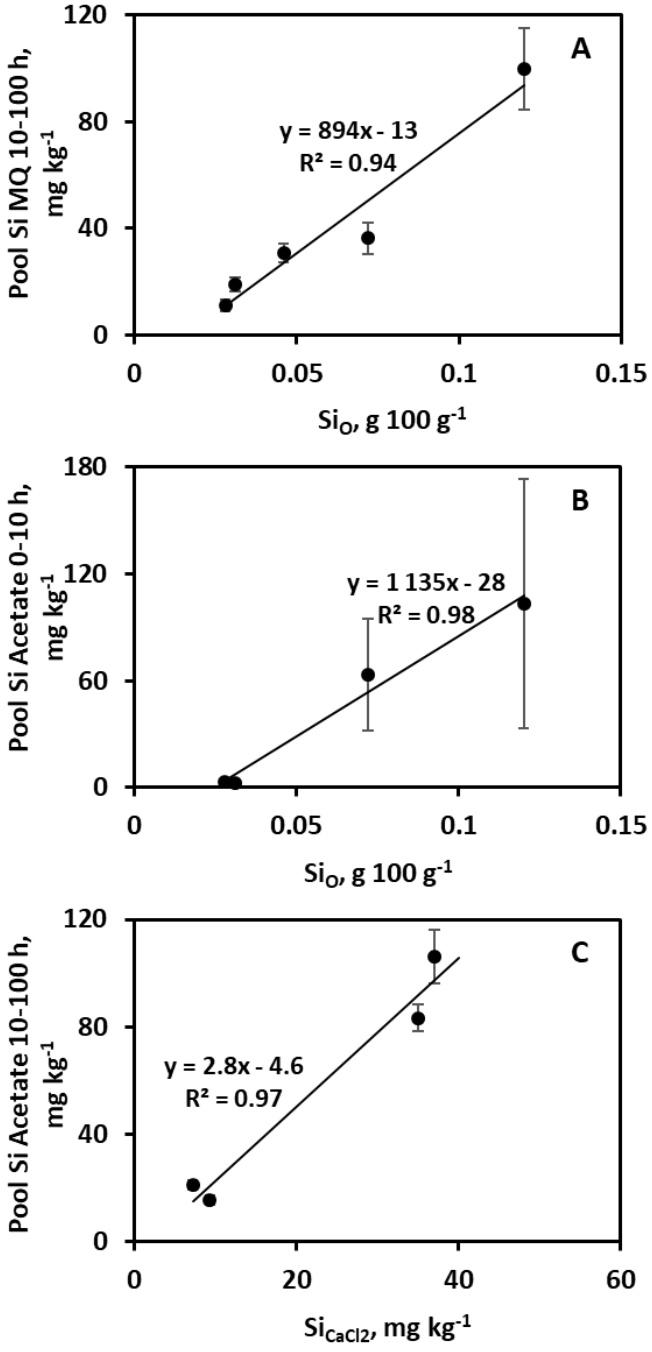

998
999
1000

1001 **Figure 6.** Correlations between pools of labile, fast-leaching Si measured in column filtration
1002 experiments in this study with different Si forms in soils reported by Cornu et al. (2022). **A:**
1003 MQ 10-100 h and Si_O, silica linked to allophane/imogolites in the form of amorphous
1004 coprecipitates with Fe/Al compounds as assessed by Tamm treatment; (**B**): acetate 0-10 h and
1005 Si_O; **C:** acetate 10-100 h versus Si_{CaCl2}, soluble bioavailable Si extracted with $CaCl_2$.

1006
1007
1008